

Autoluminescent Metal–Organic Frameworks (MOFs): Self-Photoemission of a Highly Stable Thorium MOF

Jacopo Andreo,^{*,†} Emanuele Priola,[†] Gabriele Alberto,[†] Paola Benzi,^{†,‡} Domenica Marabello,^{†,‡,§} Davide M. Proserpio,^{§,||} Carlo Lamberti,^{‡,⊥,#} and Eliano Diana^{*,†,‡,||}

[†]Department of Chemistry, University of Turin, Via Pietro Giuria 7, 10125 Turin, Italy

[‡]CriSDi, Interdepartmental Center for Crystallography, Via Pietro Giuria 7, 10125 Turin, Italy

[§]Dipartimento di Chimica, Università degli Studi di Milano, Via Golgi 19, 20133 Milano, Italy

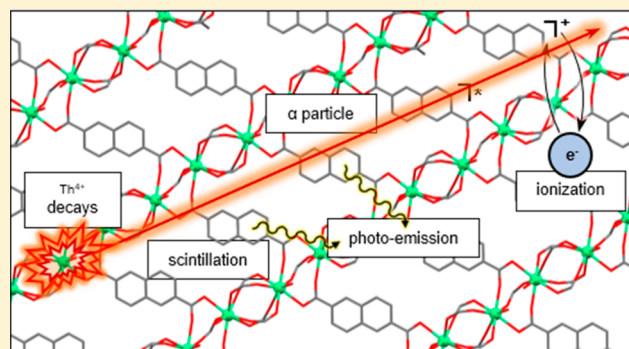
^{||}Samara Center for Theoretical Materials Science (SCTMS), Samara State Technical University, Molodogvardeyskaya St. 244, Samara 443100, Russia

[⊥]Department of Physics, Interdepartmental NIS Centre, University of Turin, Via Pietro Giuria 1, 10125 Turin, Italy

[#]The Smart Materials Research Institute, Southern Federal University, Sladkova street 178/24, Rostov-on-Don, 344090, Russia

Supporting Information

ABSTRACT: A novel thorium(IV) metal–organic framework (MOF), Th(2,6-naphthalenedicarboxylate)₂, has been synthesized via solvothermal reaction of thorium nitrate and 2,6-naphthalenedicarboxylic acid. This compound shows a new structural arrangement with an interesting topology and an excellent thermal resistance, as the framework is stable in air up to 450 °C. Most notably, this MOF, combining the radioactivity of its metal center and the scintillation property of the ligand, has been proven capable of spontaneous photon emission.



1. INTRODUCTION

Radioluminescence is one of the most fascinating properties related to radioactivity. All radioactive materials spontaneously emit photons through several physical phenomena. However, an extremely high radioactivity and sample quantity are required to make it perceivable, as most of these phenomena present low emission efficiency. The most interesting exception to this general rule is scintillation, a luminescence whose energy source is a direct ionizing particle or a high-energy photon. These interact with the scintillator (a phosphor with scintillating property) triggering multiple excitations and leading to a burst of light, whose intensity depends only on the particle nature and energy and the scintillator efficiency.¹

In the past, self-induced radioluminescent systems based on scintillation have been produced by simply mixing a strong radioactive emitter with an inorganic scintillator; however, to the best of our knowledge just one monophasic crystalline system has ever been synthesized (ThBr₄), while no metal–organic material with this feature has ever been reported. This article means to design, synthesize, and characterize a metal–organic framework (MOF) that emits photons upon the interaction between the ionizing particles produced by the metal centers and the scintillating organic linkers, i.e., autoluminescence.^{2,3}

In the past 15 years, MOFs⁴ have been drawing increasing attention due to a wide range of applications that include gas storage,⁵ adsorption,⁶ molecular sieves,⁷ catalysis,⁸ X-ray scintillation,⁹ and photocatalysis,¹⁰ leading to the synthesis of many new compounds. More recently, a promising development has been observed in the field of luminescent MOFs, aimed at the production of sensors and diodes.¹¹ Despite all the scientific and technological interest in this class of materials, until now only few studies have involved radioactive metals, none of which consider their radioactivity neither in their characterization nor in their potential applications.¹²

As shown by Allendorf and co-workers, MOFs may have scintillating properties and may be advantageous over classical organic scintillators, owing to their better resistance to the damage caused by radioactive particles. An autoluminescent MOF, besides having the same scintillating properties, would be a radiometric sensor, as its continuous emission of particles with a specific energy provides a constant internal reference.¹³

Autoluminescent MOFs featuring a porous structure may find applications as sensors, with guest species tuning the autoluminescence. Two mechanisms may be involved: (i) a decrease in luminescence, owing to the ionizing particle energy

Received: July 13, 2018

Published: October 4, 2018

loss due to interactions with the guest, and (ii) an intermolecular interaction induced tuning of the luminescent properties of the organic linkers.

To achieve a self-induced radioluminescent system, we designed a synthesis based on a new simple idea. The two MOF components may also be the two components of an autoluminescent system: a radioactive element and a scintillator.

Autoluminescence results from the interaction of the radioemitted ionizing particles with the scintillator. The mechanism is the following: (i) the scintillator is ionized by the ionizing particle; (ii) core–hole recombination takes place, leaving the system in an electronic excited state; (iii) the system decays to the ground state through visible light emission.

An appropriate metal center should not only be radioactive but also avoid interference with the luminescence of the linker. To achieve this we have chosen thorium, as (i) it emits low penetration alpha particles that release most, if not all, of their energy inside the MOF lattice, thus maximizing photo-emission; (ii) the Th^{4+} cation is a closed-shell system, which prevents charge transfer transitions and, therefore, quenching phenomena that may reduce luminescence; and (iii) its extremely low radioactivity makes thorium easier to handle than other radioactive metals. Finally, its behavior as a MOF component is well-known, yielding structures that are stable to air and water exposure. As the metal center, Th^{4+} shows three different behaviors, depending on its ligands. If bound to carboxylate ligands only, thorium shows a strong preference for the square antiprism coordination geometry, with the ions arranged in a chain-like structure and the carboxylates bridging two vertices of adjacent cations. If O^{2-} anions are also present in the structure, the metal will rather arrange in octahedral clusters of six thorium cations, bridged by eight oxygen anions, that are fairly common also in the presence of light halogen anions or complexing solvents (*N,N*-dimethylformamide or dimethyl sulfoxide). With any other type of ligand, thorium prefers an isolated metal center geometry, coordinated by 8 or 9 ligands.^{14,15}

2,6-Naphtalenedicarboxylate (NDC) was chosen as the ligand due to its proven efficiency as a scintillator. Its rigid aromatic architecture encourages luminescence emission and a rigid 3D structure, avoiding excessive flexibility and conformational freedom, which may quench or unpredictably modify the fluorescence and scintillating properties of the MOF.¹³

2. EXPERIMENTAL SECTION

Caution! Thorium nitrate ($\text{Th}(\text{NO}_3)_4 \cdot 5\text{H}_2\text{O}$) is a radioactive reactant, and suitable precautions must be followed for its handling. $\text{Th}(\text{NDC})_2$ (thorium bis-2,6-naphtalenedicarboxylate) was prepared by heating a solution of 0.1 mmol of $\text{Th}(\text{NO}_3)_4 \cdot 5\text{H}_2\text{O}$ (57.0 mg) and 0.3 mmol of 2,6-naphtalenedicarboxylic acid (2,6-NDCA) (64.8 mg) in 5 mL of *N,N*-dimethylformamide (DMF) in a 50 mL Parr autoclave at 383 K for 7 days. The resulting pale yellow crystalline powder was then centrifuged, washed three times in DMF, and dried at room temperature in air. Yield: 61.5 mg, 93.1%. This compound was also synthesized by heating a mixture of 0.1 mmol of $\text{Th}(\text{NO}_3)_4 \cdot 5\text{H}_2\text{O}$ (57.0 mg), 0.3 mmol of ligand (64.8 mg), and 5 mL of H_2O in a 50 mL Parr autoclave at 383 K for 7 days. Yield: 59.9 mg, 90.7%. The resulting yellowish powder was then centrifuged, washed three times in DMF, and dried at room temperature in air. The second method afforded suitable crystals for X-ray single-crystal diffraction. The purity of the product has been checked with elemental analysis: calculated C 43.65%, H 1.83%, O 19.38%; found C 43.2%, H 1.9%, O 19.5%.

3. RESULTS AND DISCUSSION

$\text{Th}(\text{NDC})_2$ crystallizes in the monoclinic space group $C2/c$ in the form of small prismatic crystals of pale yellow color. The structure is built by rows of octa-coordinated thorium atoms with distorted square antiprism geometry that run along the [101] direction (Figure 1). Thorium ions are bridged by four

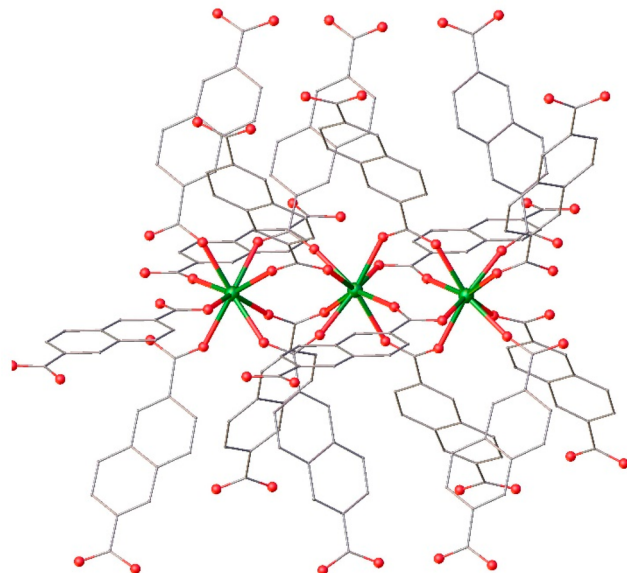


Figure 1. Rows of connected thorium atoms along the [101] direction in $\text{Th}(\text{NDC})_2$ MOF. Hydrogens are omitted for clarity. Th (green), O (red), C (gray).

carboxylate groups with variable Th–O distances in the range 2.310–2.508 Å, resulting in alternating $-\text{Th}(\text{COO})_4\text{Th}-$ bridges with Th–Th separations of 4.36 and 4.76 Å (Figure 2a). NDC molecules cross-link the metal rows, yielding a three-dimensional MOF. Triangular void channels are highlighted in the (101) view of the crystal (Figure 2b). The underlying net of the rod-MOF $\text{Th}(\text{NDC})_2$ is derived by taking the two midpoints between the Th atoms and connecting them to the carbon atoms of the carboxylate

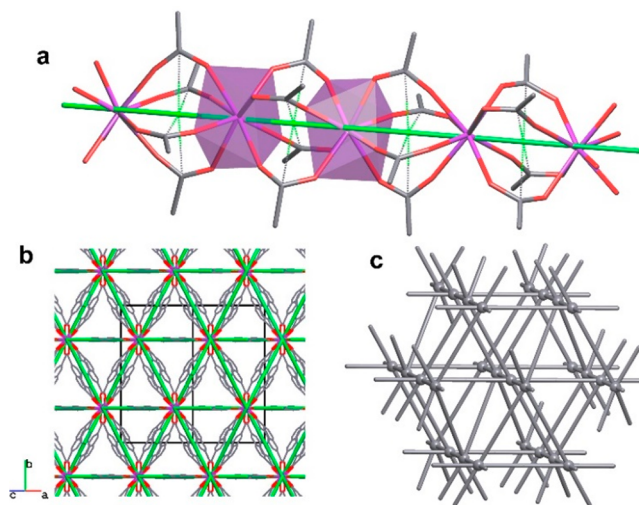


Figure 2. View of the crystal structure in the (101) plane of $\text{Th}(\text{NDC})_2$ MOF. Hydrogens are omitted for clarity.

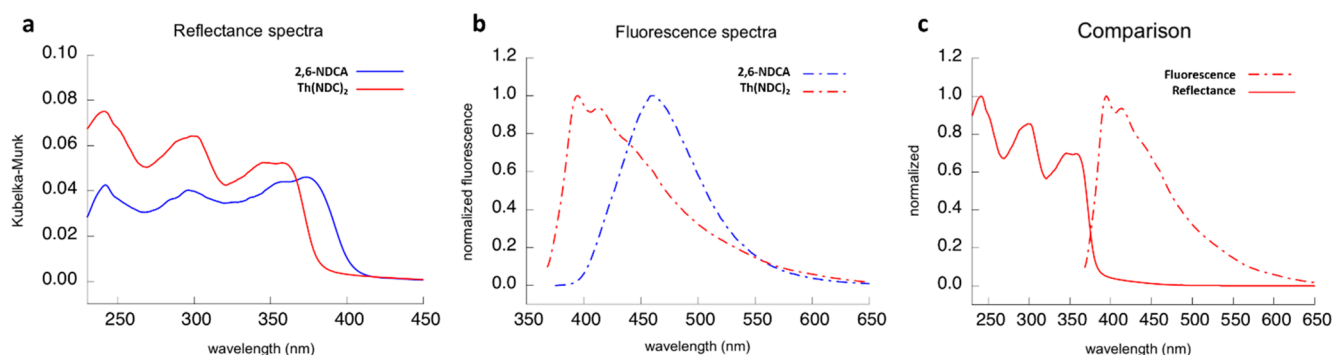


Figure 3. (a) Comparison between the reflectance spectra of the MOF and of the ligand. (b) Comparison between the fluorescence spectra of the MOF and the ligand. The wavelength of excitation is 345 nm. (c) Comparison between reflectance and fluorescence of ThNDC₂.

bridges as shown in Figure 2a, resulting in a new binodal 6-c net with point symbol $(3.4^2.5^7.6^5)(3^2.4^2.5^5.6^4.7^2)$ (Figure 2c).¹⁶ Furthermore, the view down (101) shows that the parallel rods are efficiently packed as a hexagonal lattice (Figure 2b).¹⁷ More details on the topology are available in the Supporting Information (Figures S3–S8).

The single-crystal-simulated powder X-ray diffraction pattern is comparable with the experimental powder pattern, confirming the quality of the results (Figure S9). The same figure shows a pattern collected 1 year later: the excellent agreement between the two proves that crystallinity is not damaged by either by alpha-emission or by air exposure in the medium–long time range.

Vibrational spectroscopies (Figures S10 and S11) provide a powerful tool for distinguishing between different compounds in MOF analysis. IR bands at 1655 and 451 cm^{-1} , assigned to the carboxylate group and to the metal–carboxylate bond, respectively, provide information on the success of the synthesis (Table S2 and Figures S10 and S11).¹⁸

ThNDC₂ has an excellent thermal stability: TGA analysis demonstrates that it is stable in air up to 450 °C, while the velocity of degradation has a maximum at 515 °C. The compound shows a single-step loss of 60% of weight due to the complete degradation of the organic ligands (Figure S12), the remaining 40% corresponding to thorium oxide.

Krypton absorption, performed at 77 K, shows no diffusion inside the MOF pores, with a BET of 0.41 m^2/g (Figure S13). This is due to the tilt of the NDCs on the (11–1) and (1–1–1) planes. These ligands, occluding the pores, prevent any gas absorption, despite the 22% of void that PLATON calculations predict.

Figure 3a shows the diffuse reflectance spectra of the ligand and of Th(NDC)₂. Both samples were diluted 1:20 in silica to avoid saturation in the collection of the diffuse reflectance. It is possible to observe how the MOF scaffold affects ligand absorption, resulting in a small blue-shift of the two peaks at higher wavelength. Nevertheless, the shape of the absorption spectrum is roughly the same for both Th(NDC)₂ and the ligand, indicating that the transitions are only weakly perturbed by the insertion in the MOF framework. The three transitions have been assigned, by means of TD-DFT (time-dependent density functional theory) calculations, as π to π^* . Specifically: HOMO–1 \rightarrow LUMO+1, HOMO–1 \rightarrow LUMO, HOMO \rightarrow LUMO+1, and HOMO \rightarrow LUMO for the components at 240, 300, 345, and 374 nm, respectively.

Similar considerations may be drawn about the fluorescence spectra (Figure 3b). Again, the spectrum of the MOF is blue-

shifted, with a small modification of its shape exhibiting better resolved bands. These observations are attributed to insertion in the rigid scaffold of the MOF,¹⁹ as the confinement of the ligand results in its impossibility to decay in certain vibronic states. This implies that the remaining transitions became more distant in energy, thus resulting in a better resolved spectrum.

Figure 3c shows the normalized absorbance and fluorescence spectra of the MOF. The two spectra present only a small overlap, which results in a very small contribution of self-absorption to the fluorescence quenching. Moreover, if we consider that a scintillation spectrum is red-shifted compared to the fluorescence one, this contribution becomes negligible in terms of scintillation quenching and thus in terms of autoluminescence.^{1,13}

Absolute quantum yield was also measured on solid samples by coupling Quanta ϕ to a Horiba Jobin Yvon Fluorolog 3 equipped with a 450 W xenon lamp and a R928 photomultiplier. In the case of the MOF a value of 39.84% ($\pm 3\%$) was calculated, whereas a photoemission efficiency of 34.5 ($\pm 3\%$) was obtained for the organic ligand in the same experimental conditions. These data are in good agreement with those obtained by steady state fluorescence measurements, indicating an increase in the probability of the radiative decay process with respect to nonradiative ones due to the loss of molecular degrees of freedom experienced by the ligand constrained in the MOF scaffold.

Fluorescence lifetimes were measured using a time-correlated single photon counting (TCSPC) technique (Horiba Jobin Yvon) with excitation source NanoLed at 297 nm (Horiba) or at 370 nm (Horiba) and impulse repetition rate of 1 MHz at 90° to a TBX-4 detector. The detector was set to the maximum of emission for the compound in the exam, with a 5 nm band pass. The instrument was set in the Reverse TAC mode, where the first detected photon represented the start signal by the time-to-amplitude converter (TAC) and the excitation pulse triggered the stop signal. DAS6 decay analysis software was used for lifetime calculation. Both the ligand and the MOF show a decay composed by three different lifetimes (NDC: τ 13.56 ns, 10%; τ 211.23 ns, 49%; τ 323.13 ns, 41%; χ^2 1.07; Th(NDC)₂: τ 10.63 ns, 83%; τ 22.84 ns, 9%; τ 314.09 ns, 8%; χ^2 1.16). These data apparently appear in contrast with the quantum yields, as the ligand shows much longer lifetimes. This discrepancy, however, is easily explained by the crystalline habit of the two materials: the NDC is characterized by strong π interactions that lead to the formation of excitons that prolong the lifetimes while quenching the fluorescence. On the contrary, the MOF

topologies do not allow the formation of π stacking among ligands, thus shortening the lifetimes and removing the quench associated with this phenomenon.

With the aim of evaluating the self-induced radioluminescence, we employed a Packard Tri-Carb 2200 CA liquid scintillator. This instrument uses two photomultiplier tubes connected to a coincidence circuit to detect the light pulses resulting from the scintillation response of a scintillator to an ionizing particle. This results in a high sensitivity because this setup minimizes false signals from the photomultiplier tubes arising from the dark current. Since the instrument normally works on liquid solutions, we modified the standard procedure by placing a capillary tube with a diameter of 0.4 mm, bearing a known quantity of the sample, in the center of the vial employed by the instrument (Figure S14).

Initially, we determined the background signal of the instrument, using a tube filled with a radioactive compound: recrystallized NaF was found suitable for this, as both its elements present a unique stable isotope with a natural abundance of 100%. Using this setup, the instrumental noise was determined at 31 counts per minute (c.p.m.), independently of the mass sample, and this value was subtracted from any raw data collected with this instrumental protocol.

The 2,6-naphthalendicarboxylic acid performed similarly, with results comparable to the base value. $\text{Th}(\text{NO}_3)_4 \cdot 5\text{H}_2\text{O}$ yielded 10.9 counts per minute per milligram (0.42 mg of thorium). This value corresponds roughly to 10% of the particles emitted by the thorium. $\text{Th}(\text{NDC})_2$ has a count per minute per milligram (0.35 mg of thorium) ratio of 173.0, meaning that roughly 200% of the ionizing particles that are emitted produce enough photons to be detected, resulting in a 20-fold enhancement of the autoluminescence. This value exceeds 100% because the scintillation counter usually works with aqueous solutions of organic scintillators, which present a much faster recombination of the ionized states induced by ionizing particles, compared to a solid system. This implies that the flash of photons emitted by the MOF, when it interacts with an ionizing particle, is sensibly longer than the one produced by the liquid scintillator. For this reason, the instrument recognizes every burst of the MOF as two separate events, doubling the count. The measurements on a mixture of $\text{Th}(\text{NO}_3)_4 \cdot 5\text{H}_2\text{O}$ and 2,6-NDCA in a ratio of 1:2 grinded separately and then mixed together to avoid a solid-state reaction, resulting in a count equivalent to 168% of the particles emitted, meaning that only 84% of the decay events of the thorium may be revealed by the simple mixture of the two MOF components. This proves that a mixing at the molecular level and a crystalline structure strongly improve the autoluminescent properties of the system. This is even more interesting when combined with the resilience of the MOF to the damage inflicted by the particles emitted by the thorium centers: as the MOF crystallinity is unaffected after one year, similarly its autoluminescence count does not vary.

To further prove that the instrument response is triggered only by the MOF's autoluminescence two additional experiments were designed and performed. The first was carried out by submerging the capillary in a liquid scintillator (Ultima Gold AB, from PerkinElmer, SP8S3), thus avoiding the presence of air in the vial, which could interact with the alpha particles that could leave the capillary, and the beta particles originated from thorium's family decay (that are very few because the members of the decay chain did not have enough time to reach the equilibrium). The photon counter, as

expected, improved, but the profile of the particle detection of this system shows two distinct peaks: one analogous to that of the MOF and one relative to the liquid scintillator (Figure 4).

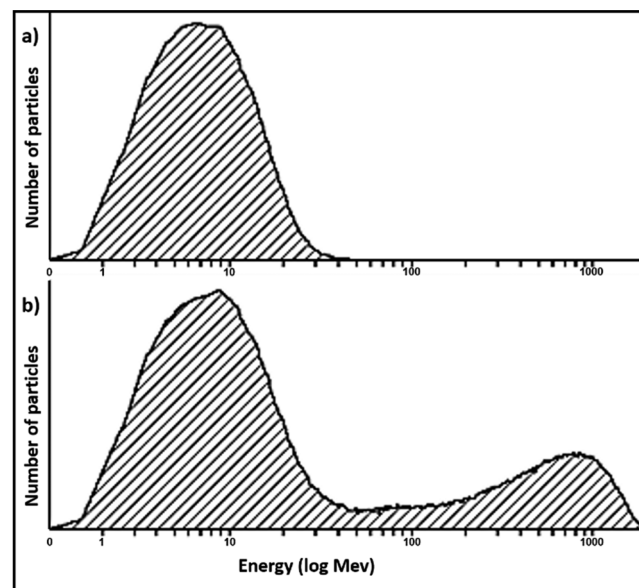


Figure 4. (a) Energy profile of the particle detection of pure $\text{Th}(\text{NDC})_2$. (b) Energy profile of the particle detection of the MOF submerged in the liquid scintillator.

The second experiment was aimed at proving that the instrumental signal was not generated by γ rays. To do this, we simply wrapped the capillary in black paper, as it can block most of the visible and UV light but is transparent to photons with higher energies. With this setup, the particle counter dropped to 16.8 per minute per milligram, proving that the measurements reported in Figure 4 are not influenced by gamma-rays.

We have also tested for autoluminescence two thorium MOFs whose ligands present fluorescence but not scintillation. For this purpose, we chose $\text{Th}_2(\text{bdc})_4(\text{DMF})_4$ and $\text{Th}_6\text{O}_4(\text{OH})_4(\text{H}_2\text{O})_6(\text{bdc})_6 \cdot 6\text{DMF} \cdot 12\text{H}_2\text{O}$, and both use benzene-1,4-dicarboxylate as ligand; however, the second presents the octahedral thorium cluster as metal centers and has a 1:1 stoichiometry between the ligand and the metal.¹⁴ $\text{Th}_2(\text{bdc})_4(\text{DMF})_4$ has a normalized c.p.m. of 47.7 and has a thorium to compound ratio of 0.32, meaning that 61% of alpha particles have been detected (30.5 if we account for the doubling of the counts for solid-state systems). $\text{Th}_6\text{O}_4(\text{OH})_4(\text{H}_2\text{O})_6(\text{bdc})_6 \cdot 6\text{DMF} \cdot 12\text{H}_2\text{O}$ presents a normalized c.p.m. of 41.6. As in one milligram of compound 0.42 mg is of thorium, it has 41% of particle detection (20.5% corrected for the solid state). Not surprisingly these values are higher than the one of thorium nitrate, as the fluorescence of the compound may still be triggered by the energy of the alpha particles, but their efficiency is still far from the one of $\text{Th}(\text{NDC})_2$, with its scintillating ligand.

4. CONCLUSIONS

To summarize, this work presents a thorium MOF, with a novel structure and a complex new topology. Remarkably (see SI), the MOF is stable up to 450 °C in air, and its framework is not affected by aging (in a one-year scale). Furthermore, we proved how this MOF, combining the alpha-particle emission

typical of thorium with the scintillating properties of the 2,6-naphthalenedicarboxylate, spontaneously emits photons, resulting in the first autoluminescent MOF. Finally, this is the first reported case of a metal–organic framework with a property directly connected with the radioactivity of its metal center. These two factors prove that rational design leads to new and exotic properties in MOFs, properties that may be linked to uncommon or unfashionable sources, in this case radioactivity. What is certain is that we are only beginning to explore an exciting new area of chemistry and functional materials.

■ ASSOCIATED CONTENT

Supporting Information

The Supporting Information is available free of charge on the ACS Publications website at DOI: 10.1021/jacs.8b07113.

CIF file for C24 H12 O8 Th (CIF)

X-ray Structure determination and structural data, X-ray powder patterns, computational details, IR and Raman spectra, thermogravimetric curve (PDF)

■ AUTHOR INFORMATION

Corresponding Authors

*Prof. Eliano Diana. E-mail: eliano.diana@unito.it

*Jacopo Andreo. E-mail: jacopo.andreo@studenti.unipr.it

ORCID

Domenica Marabello: 0000-0002-9648-7735

Davide M. Proserpio: 0000-0001-6597-9406

Carlo Lamberti: 0000-0001-8004-2312

Eliano Diana: 0000-0002-7345-8501

Notes

The authors declare no competing financial interest.

■ ACKNOWLEDGMENTS

We thank Prof. Alessandro Lo Giudice, Dr. Francesca Peccati, and Eugeny V. Alexandrov for useful suggestions and discussions. C.L. acknowledges the mega-grant of Ministry of Education and Science of the Russian Federation (14.Y26.31.0001).

■ ABBREVIATIONS

MOF	Metal–organic Framework;
NDC	2,6-naphthalenedicarboxylate;
2,6-NDCA	2,6-naphthalenedicarboxylic acid;
DMF	<i>N,N</i> -dimethylformamide;
Th(NDC) ₂	thorium bis-2,6-naphthalenedicarboxylate;
TD-DFT	time-dependent density functional theory;
TCSPC	time-correlated single photon counting;
TAC	time-to-amplitude converter;
c.p.m.	counts per minute;

■ REFERENCES

- (1) (a) Birks, J. B. *The theory and practice of scintillation counting*; Pergamon Press, 1964. (b) Blasse, G. *Chem. Mater.* **1994**, *6*, 1465–1475. (c) Milbrath, B. D.; Peurrung, A. J.; Bliss, M.; Weber, W. J. *J. Mater. Res.* **2008**, *23*, 2561–2581. (d) Nikl, M.; Yoshikawa, A. *Adv. Opt. Mater.* **2015**, *3*, 463–481.
- (2) (a) Carlier, R.; Genet, M. *Comp. Rend. C* **1975**, *281*, 671. (b) Genet, M.; Hussonnois, M.; Krupa, J. C.; Carlier, R.; Guillaumont, R. *J. Lumin.* **1976**, *12*, 953. (c) Carlier, R.; Krupa, J. C.; Hussonnois, M.; Genet, M.; Guillaumont, R. *Nucl. Instrum. Methods* **1977**, *143*, 613–615.

- (4) (a) Yaghi, O. M.; O’Keeffe, M.; Ockwig, N. W.; Chae, H. K.; Eddaoudi, M.; Kim, J. *Nature* **2003**, *423*, 705–714. (b) Furukawa, H.; Cordova, K. E.; O’Keeffe, M.; Yaghi, O. M. *Science* **2013**, *341*, 974. (c) Batten, S. R.; Champness, N. R.; Chen, X.-M.; Garcia-Martinez, J.; Kitagawa, S.; Öhrström, L.; O’Keeffe, M.; Paik Suh, M.; Reedijk, J. *CrystEngComm* **2012**, *14*, 3001–3004.

- (5) (a) Morris, R. E.; Wheatley, P. S. *Angew. Chem., Int. Ed.* **2008**, *47* (27), 4966–4981. (b) Ma, S. Q.; Zhou, H. C. *Chem. Commun.* **2010**, *46* (1), 44–53. (c) Dinca, M.; Yu, A. F.; Long, J. R. *J. Am. Chem. Soc.* **2006**, *128* (27), 8904–8913. (d) Millward, A. R.; Yaghi, O. M. *J. Am. Chem. Soc.* **2005**, *127* (51), 17998–17999. (e) Eddaoudi, M.; Kim, J.; Rosi, N.; Vodak, D.; Wachter, J.; O’Keeffe, M.; Yaghi, O. M. *Science* **2002**, *295*, 469–472.

- (6) (a) Li, J. R.; Kuppler, R. J.; Zhou, H. C. *Chem. Soc. Rev.* **2009**, *38* (5), 1477–1504. (b) Sumida, K.; Rogow, D. L.; Mason, J. A.; McDonald, T. M.; Bloch, E. D.; Herm, Z. R.; Bae, T. H.; Long, J. R. *Chem. Rev.* **2012**, *112* (2), 724–781.

- (7) Li, J.-R.; Sculley, J.; Zhou, H.-C. *Chem. Rev.* **2012**, *112*, 869–932.

- (8) (a) Lee, J.; Farha, O. K.; Roberts, J.; Scheidt, K. A.; Nguyen, S. T.; Hupp, J. T. *Chem. Soc. Rev.* **2009**, *38* (5), 1450–1459. (b) Corma, A.; Garcia, H.; Xamena, F. *Chem. Rev.* **2010**, *110* (8), 4606–4655. (c) Vermeulen, N. A.; Karagiari, O.; Sarjeant, A. A.; Stern, C. L.; Hupp, J. T.; Farha, O. K.; Stoddart, J. F. *J. Am. Chem. Soc.* **2013**, *135*, 14916–14919. (d) Butova, V. V.; Soldatov, M. A.; Guda, A. A.; Lomachenko, K. A.; Lamberti, C. *Russ. Chem. Rev.* **2016**, *85*, 280–307. (e) Rogge, S. M. J.; Bavykina, A.; Hajek, J.; Garcia, H.; Olivoso-Suarez, A. I.; Sepúlveda-Escribano, A.; Vimont, A.; Clet, G.; Bazin, P.; Kapteijn, F.; Daturi, M.; Ramos-Fernandez, E. V.; Llabrés i Xamena, F. X.; Van Speybroeck, V.; Gascon, J. *Chem. Soc. Rev.* **2017**, *46*, 3134–3184.

- (9) Wang, Y.; Yin, X.; Liu, W.; Xie, J.; Chen, J.; Silver, M. A.; Sheng, D.; Chen, L.; Diwu, J.; Liu, N.; Chai, Z.; Thomas, P.; Albrecht-Schmitt, E.; Wang, S. *Angew. Chem., Int. Ed.* **2018**, *57*, 7883–7887.

- (10) Zhang, T.; Lin, W. *Chem. Soc. Rev.* **2014**, *43*, 5982–5993.

- (11) (a) Dou, Z.; Yu, J.; Cui, Y.; Yang, Y.; Wang, Z.; Yang, D.; Qian, G. *J. Am. Chem. Soc.* **2014**, *136*, 5527–5530. (b) Bauer, C. A.; Timofeeva, T. V.; Settersten, T. B.; Patterson, B. D.; Liu, B. A.; Simmons, V. H.; Allendorf, M. D. *J. Am. Chem. Soc.* **2007**, *129*, 7136–7144. (c) Heine, J.; Muller-Buschbaum, K. *Chem. Soc. Rev.* **2013**, *42*, 9232–9242. (d) Kreno, L. E.; Leong, K.; Farha, O. K.; Allendorf, M.; Van Duyen, R. P.; Hupp, J. T. *Chem. Rev.* **2012**, *112*, 1105–1125.

- (12) (a) Wang, Y.; Liu, Z.; Li, Y.; Bai, Z.; Liu, W.; Wang, Y.; Xu, X.; Xiao, C.; Sheng, D.; Diwu, J.; Su, J.; Chai, Z.; Albrecht-Schmitt, T. E.; Wang, S. *J. Am. Chem. Soc.* **2015**, *137*, 6144–6147. (b) Xie, J.; Wang, Y.; Liu, W.; Yin, X.; Chen, L.; Zou, Y.; Diwu, J.; Chai, Z.; Albrecht-Schmitt, T. E.; Liu, G.; Wang, S. *Angew. Chem., Int. Ed.* **2017**, *56*, 7500–7504. (c) Liu, H.; Xu, C.; Li, D.; Jiang, H. L. *Angew. Chem., Int. Ed.* **2018**, *57*, 5379–5383. (d) Li, P.; Vermeulen, N. A.; Malliakas, C. D.; Gómez-Gualdrón, D. A.; Howarth, A. J.; Mehdi, B. L.; Dohnalkova, A.; Browning, N. D.; O’Keeffe, M.; Farh, O. K. *Science* **2017**, *356*, 624–627.

- (13) (a) Cui, Y.; Yue, Y.; Qian, G.; Chen, B. *Chem. Rev.* **2012**, *112*, 1126–1162. (b) Doty, F. P.; Bauer, C. A.; Skulan, A. J.; Grant, P. G.; Allendorf, M. D. *Adv. Mater.* **2009**, *21*, 95–101. (c) Perry, J. J.; IV; Feng, P. L.; Meek, S. T.; Leong, K.; Doty, F. P.; Allendorf, M. D. *J. Mater. Chem.* **2012**, *22*, 10235–10248. (d) Mathis, S. R.; II; Golafale, S. T.; Bacsa, J.; Steiner, A.; Ingram, C. W.; Doty, F. P.; Audene, E.; Hattare, K. *Dalton Trans.* **2017**, *46*, 491–500. (e) Mathis, S. R.; II; Golafale, S. T.; Solntsev, K. M.; Ingram, C. W. *Crystals* **2018**, *8*, 53.

- (14) Falaise, C.; Charles, J. S.; Volkringer, C.; Loiseau, T. *Inorg. Chem.* **2015**, *54*, 2235–2242.

- (15) (a) Falaise, C.; Volkringer, C.; Loiseau, T. *Inorg. Chem. Commun.* **2014**, *39*, 26–30. (b) Ok, K. M.; Sung, J.; Hu, G.; Jacobs, R. M. J.; O’Hare, D. *J. Am. Chem. Soc.* **2008**, *130*, 3762–3763. (c) Kim, J.-Y.; Norquist, A.; O’Hare, D. *J. Am. Chem. Soc.* **2003**, *125*, 12688–12689. (d) Ok, K. M.; O’Hare, D. *Dalton Trans.* **2008**, *41*, 5560. (e) Ramaswamy, P.; Prabhu, R.; Natarajan, S. *Inorg. Chem.* **2010**, *49*, 7927–7934. (f) Thuéry, P. *Eur. J. Inorg. Chem.* **2014**, *58*–68. Thuéry, P. *Inorg. Chem.* **2011**, *50*, 1898–1904. (g) Li, Y.; Yang, Z.; Wang, Y.;

Bai, Z.; Zheng, T.; Dai, X.; Liu, S.; Gui, D.; Liu, W.; Chen, M.; Chen, L.; Diwu, J.; Zhu, L.; Zhou, R.; Chai, Z.; Albrecht-Schmitt, T. E.; Wang, S. *Nat. Commun.* **2017**, *8*, 1354.

(16) (a) Alexandrov, E. V.; Blatov, V. A.; Proserpio, D. M. *CrystEngComm* **2011**, *13*, 3947–3958. (b) Schoedel, A.; Li, M.; Li, D.; O’Keeffe, M.; Yaghi, O. M. *Chem. Rev.* **2016**, *116*, 12466–12535.

(17) (a) O’Keeffe, M.; Andersson, S. *Acta Crystallogr., Sect. A: Cryst. Phys., Diffr., Theor. Gen. Crystallogr.* **1977**, *33*, 914–923. (b) Rosi, N. L.; Kim, J.; Eddaoudi, M.; Chen, B.; Yaghi, O. M. *J. Am. Chem. Soc.* **2005**, *127*, 1504–1518.

(18) Bonino, F.; Lamberti, C.; Bordiga, S. IR and Raman Spectroscopies Probing MOFs Structure, Defectivity, and Reactivity. In *The Chemistry of Metal–Organic Frameworks: Synthesis, Characterization, and Applications*; Kaskel, S., Ed.; Wiley-VCH: Weinheim, 2016; Vol. 22, pp 657–690.

(19) Wei, Z.; Gu, Z. Y.; Arvapally, R. K.; Chen, Y. P.; McDougald, R. N., Jr.; Ivy, J. F.; Yakovenko, A. A.; Feng, D.; Omary, M. A.; Zhou, H. C. *J. Am. Chem. Soc.* **2014**, *136*, 8269–8276.